**A GAMMA-RAY PERSPECTIVE FROM LUNAR PROSPECTOR.** O. Gasnault[1], R.C. Elphic[2], D.J. Lawrence[3], S. Karunatillake[4], C. d'Uston[1], and O. Forni[1], [1]Centre d'Etude Spatiale des Rayonnements, Université Paul Sabatier, CNRS (9 av. C. Roche, 31400 Toulouse, France; gasnault@cesr.fr), [2]Space Science & Applications (Los Alamos National Laboratory, NM, USA), [3]Applied Physics Laboratory (Johns Hopkins University, Laurel, MD, USA), [4]Department of Astronomy (Cornell University, Ithaca, NY,USA).

**Introduction:** The primary crust of the Moon formed early in its history, was disrupted by large impacts, partially resurfaced by mare basalts (secondary crust), and has undergone impact cratering and space weathering over eons. The first global investigation by Clementine and Lunar Prospector (LP) and the continued analysis of the mission-returned samples led to a major review of the state of the art of lunar science [1]. The four new orbital missions (Kaguya, Chang'e, Chandrayaan-1, and Lunar Reconnaissance Orbiter) will provide new opportunities for a better understanding of the diversity of the lunar surface through a complete mapping with better spatial coverage and resolution than ever before.

Each instrumental technique returns complementary information necessary for a comprehensive interpretation. For example, the regolith composition is used to define and characterize the surface units that result from the extensive differentiation, and from the petrological and mechanical processes. Here we propose to build on the elemental composition maps derived from gamma-ray spectroscopy (GRS) aboard LP [2] and data processing methods developed for the Mars Odyssey GRS [3] to outline provinces that can be further investigated by the new missions, especially by the instruments sensitive to the elemental composition such as the Kaguya GRS [4], and the Chandrayaan-1 X-ray and high-energy spectrometers [5, 6].

**Methods for Province Identification:** The LP-GRS returned abundances of iron and thorium integrated over ~1 m of regolith depth with a spatial resolution (FWHM) of ~80 km [7, 8] and many more elements (Mg, Al, Si, Ca, Ti, K) with a coarser resolution of ~150 km [9]. The large dynamic range in lunar compositions at the scale of tens or hundreds of kilometers makes it relatively easy to distinguish the various terranes. By combining various observations it is possible to map petrologic units [10] or, at larger scale, major terranes of different lithologies such as the Procellarum KREEP, the feldspathic highlands, and the South Pole-Aitken terranes [11].

Two major methods are proposed here: the deviation from the mean, and a multivariate analysis.

*Deviation from the mean.* The simplest thing to do is to work on a single map, compute the global mean composition, and search for deviations from the average value that are significant, i.e. deviations larger than the standard error of the data (sigma: σ). A Student T-test can be used for that purpose [12, 13]. In Fig. 1 the contours delineate the regions with an excess of thorium at the surface of the Moon using that technique. We assumed the largest error between a systematic relative error of 10% and a Poisson uncertainty given by 0.27-2.4E-5*(latitude^2) µg/g [14].

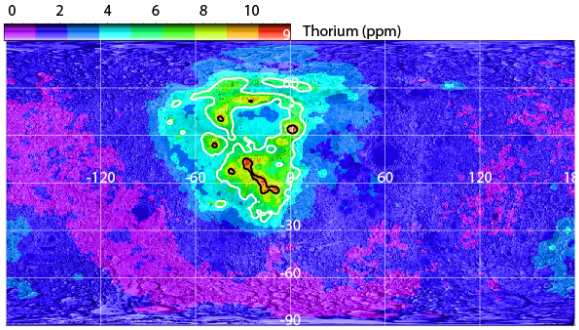


**Figure 1:** Lunar regolith thorium content (overall average = 1.58 µg/g and standard deviation = 1.85 µg/g). The black and white contours delineate the regions that are respectively 4 and 2 sigmas richer in thorium than average.

Another simple approach to identify end-member compositions is based on a scatter plot of the abundances of two elements. The case of iron and thorium epitomizes this for the Moon at global scale, as shown in Fig. 2. At least three major typical compositions are visible: the feldspathic highlands (low-FeO, low-Th), the mare basalts (high-FeO, low-Th), and the KREEP-bearing materials (high-Th).

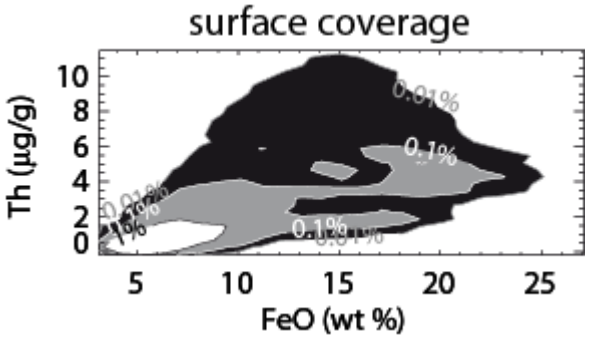


**Figure 2:** Density plot of Th *vs.* Fe from LP-GRS.

*Multivariate statistical analysis.* To illustrate this type of analysis we will use the LP-GRS data from [9] with a spatial resolution of 150 km and assume a systematic relative error of 10%.

The deviation from the mean method applied to one or two elements can be generalized to all the elements simultaneously to only retain the regions where several element abundances deviate significantly from the mean [15]. For example Fig. 3 highlights a basaltic region where iron and titanium abundances are above the global means by 2-σ and aluminum is 2- σ below its global mean. While the mare basalt regions can be defined by high iron contents (and low aluminum contents), titanium is often used to classify the various lunar basalts [e.g. 16]. Some of these basalts are significantly enriched (above 2- σ) in thorium and potassium (white contours), which may also reflect a different genesis. Note that this method is actually most helpful when the abundance distributions are close to be Gaussian, which is not the case here.

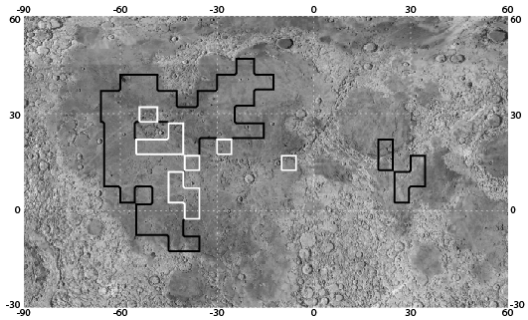


**Figure 3.** Moon's nearside. The black contours show the regions enriched in Fe and Ti and depleted in Al. Within the white contours, they are also enriched in Th and K.

Another multivariate approach is based on Principal Component Analysis applied to all available maps that returns an optimal linear combination of the elements. One can extract the two first principal components, which yield the maximum variance of composition, to generate a scatter plot as in Fig. 2 [e.g., 17] or to search for groups of data points within all the dimensions through clustering analysis [e.g., 18]. By definition, cluster of data points are compositionally close; these clustered data define a geochemical province if they map in a continuous area. This approach is illustrated in Fig. 4 where five provinces are defined in a preliminary analysis: the highlands are represented by provinces #1 and #3, with some differences in magnesium, thorium, and potassium; the mare of the Procellarum KREEP terrane are represented by province #4; province #5 is characterized by enrichment in KREEP materials, while province #2 has an intermediate composition.

**Provinces of Interest for Further Investigations:** Besides the hydrated polar regions [19] and the dehydrated equatorial regions [20] revealed by the LP Neutron Spectrometer, a few provinces can be pointed here with a gamma-ray perspective. Fig. 1 shows some thorium "hot spots" listed by [7], e.g. at 100.5E, 60.9N in the Compton-Belkovich region, which might be an evolved lithology. Fig. 2 and 3 reveal some basalts with high-FeO and intermediate thorium contents that are located in the maria of Oceanus Procellarum and may have a particular origin [21]. Fig. 4 shows the South Pole Aitken Terrane with a mix of compositions shown in purple and dark blue, the latest being intermediate between typical highlands (light blue) and typical mare basalts (green).

Finally the Lunar International Science Calibration/Coordination Targets [22] are shown as black boxes in Fig. 4; note that they all fall in different clusters and thus represent different compositions detectable by gamma-ray or X-ray spectroscopy.

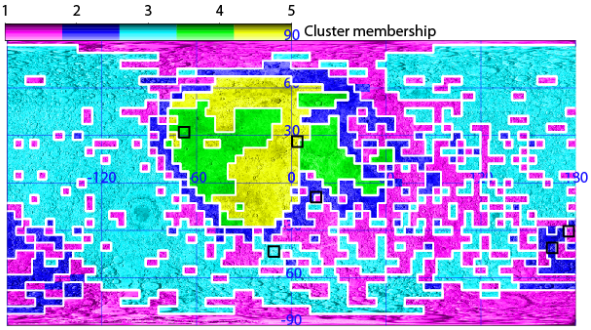


**Figure 4:** Five lunar provinces. Each color represents a relatively uniform composition distinct from the others.

**References:** [1] New Views of the Moon (2006), *Reviews in Mineralogy and Geochemistry, 60*. [2] Lawrence et al. (1998) *Science, 281,* 1484–1489. [3] Boynton et al. (2007) *J. Geophys. Res., 112, E12S99*. [4] *Kobayashi et al.,* these proceedings. [5] Joy et al. (2008) *LPS XXXIX,* Abstract #1070. [6] Gasnault (2004) *Int. Conf. on Exploration and Utilization of the Moon,* Abstract #37. [7] Lawrence et al. (2003) *J. Geophys. Res., 108(E9),* 5102. [8] Lawrence et al. (2002) *J. Geophys. Res., 107(E12),* 5130. [9] Prettyman et al. (2006) *J. Geophys. Res., 111,* E12007. [10] Spudis (2000) *LPS XXXI,* Abstract #1414. [11] Jolliff et al. (2000) *J. Geophys. Res., 105,* 4197–4216. [12] Keller et al. (2006) *J. Geophys Res., 111,* E03S08. [13] Taylor et al. (2006) *J. Geophys. Res., 111,* E03S06. [14] Lawrence et al. (2000) *J. Geophys. Res., 105(E8),* 20,307-20,331. [15] Karunatillake et al. (2007) *7th Int. Conf. on Mars,* Abstract #3190. [16] Giguere et al. (2000) *Meteorit. Planet. Sci., 35*, 193-200. [17] Chevrel et al. (2002) *J. Geophys. Res., 107(E12),* 5132. [18] Gasnault et al. (2006) *EGU General Assembly 3rd*, Abstract #06-A-07690. [19] Feldman et al. (2001) *J. Geophys. Res., 106 (E10),* 23,231-23,251. [20] Maurice et al. (2001) *LPS XXXII,* Abstract #2033. [21] Gasnault et al. (2002) *LPS XXXIII,* Abstract #2010. [22] Pieters et al. (2006) *LPS XXXVIII,* Abstract #1295.